



HAL
open science

Immunogenicity and efficacy of heterologous ChAdOx1-BNT162b2 vaccination

Bruno Pozzetto, Vincent Legros, Sophia Djebali, Véronique Barateau, Nicolas Guibert, Marine Villard, Loïc Peyrot, Omran Allatif, Jean-Baptiste Fassier, Amélie Massardier-Pilonchery, et al.

► **To cite this version:**

Bruno Pozzetto, Vincent Legros, Sophia Djebali, Véronique Barateau, Nicolas Guibert, et al.. Immunogenicity and efficacy of heterologous ChAdOx1-BNT162b2 vaccination. *Nature*, 2021, 600 (7890), pp.701-706. 10.1038/s41586-021-04120-y . hal-03773083

HAL Id: hal-03773083

<https://hal.science/hal-03773083>

Submitted on 9 Jan 2024

HAL is a multi-disciplinary open access archive for the deposit and dissemination of scientific research documents, whether they are published or not. The documents may come from teaching and research institutions in France or abroad, or from public or private research centers.

L'archive ouverte pluridisciplinaire **HAL**, est destinée au dépôt et à la diffusion de documents scientifiques de niveau recherche, publiés ou non, émanant des établissements d'enseignement et de recherche français ou étrangers, des laboratoires publics ou privés.

Immunogenicity and efficacy of heterologous ChAdOx1–BNT162b2 vaccination

<https://doi.org/10.1038/s41586-021-04120-y>

Received: 19 July 2021

Accepted: 10 October 2021

Published online: 21 October 2021

 Check for updates

Bruno Pozzetto^{1,2,8}, Vincent Legros^{1,3,8}, Sophia Djebali^{1,8}, Véronique Barateau^{1,8}, Nicolas Guibert⁴, Marine Villard¹, Loïc Peyrot¹, Omran Allatif¹, Jean-Baptiste Fassier⁴, Amélie Massardier-Pilonchéry⁴, Karen Brenzel-Pesce⁵, Melyssa Yaugel-Novoa^{1,2}, Solène Denolly¹, Bertrand Boson¹, Thomas Bourlet¹, Antonin Bal^{1,6}, Martine Valette⁶, Thibault Andrieu⁷, Bruno Lina^{1,6}, Covid-Ser study group*, François-Loïc Cosset^{1,9,10}, Stéphane Paul^{1,2,9,10}, Thierry Defrance^{1,9,10}, Jacqueline Marvel^{1,9,10}, Thierry Walzer^{1,9,10} & Sophie Trouillet-Assant^{1,5,9,10}

Following severe adverse reactions to the AstraZeneca ChAdOx1-S-nCoV-19 vaccine^{1,2}, European health authorities recommended that patients under the age of 55 years who received one dose of ChAdOx1-S-nCoV-19 receive a second dose of the Pfizer BNT162b2 vaccine as a booster. However, the effectiveness and the immunogenicity of this vaccination regimen have not been formally tested. Here we show that the heterologous ChAdOx1-S-nCoV-19 and BNT162b2 combination confers better protection against severe acute respiratory syndrome coronavirus 2 (SARS-CoV-2) infection than the homologous BNT162b2 and BNT162b2 combination in a real-world observational study of healthcare workers ($n = 13,121$). To understand the underlying mechanism, we conducted a longitudinal survey of the anti-spike immunity conferred by each vaccine combination. Both combinations induced strong anti-spike antibody responses, but sera from heterologous vaccinated individuals displayed a stronger neutralizing activity regardless of the SARS-CoV-2 variant. This enhanced neutralizing potential correlated with increased frequencies of switched and activated memory B cells that recognize the SARS-CoV-2 receptor binding domain. The ChAdOx1-S-nCoV-19 vaccine induced a weaker IgG response but a stronger T cell response than the BNT162b2 vaccine after the priming dose, which could explain the complementarity of both vaccines when used in combination. The heterologous vaccination regimen could therefore be particularly suitable for immunocompromised individuals.

The ChAdOx1-S-nCoV-19 and BNT162b2 vaccines (hereafter referred to as ChAd and BNT, respectively) have been shown to confer strong protection against SARS-CoV-2 infection and to induce robust immune responses directed against the spike protein of SARS-CoV-2 when administered in a homologous setting^{3–5}. However, the effectiveness of a ChAd–BNT combination as a prime–boost regimen has not been formally tested in vaccine trials. To compare the risk of SARS-CoV-2 infection following heterologous ChAd–BNT or homologous BNT–BNT vaccination schedules, we extracted data from the occupational medicine database of the University Hospital of Lyon (Hospices Civils de Lyon), France. Specifically, we analysed the number of individuals who received each vaccination regimen (which started in January 2021 in both groups) and the number of SARS-CoV-2 infections (documented by a positive

PCR with reverse transcription (RT–PCR) result) that occurred at least 2 weeks after the booster dose in each group (Table 1). Ten infections were identified out of 2,512 individuals (0.40%) in the heterologous vaccination group compared with 81 infections out of 10,609 individuals (0.76%) in the homologous vaccination group (Fig. 1). As the age of the individual and the vaccination regimen are known covariates, we used a multiple logistic regression model to model the probability of being infected. Our predictors were age (set as a continuous variable, considered as a possible confounder) and the vaccination regimen. Results showed that age is not associated with infection status ($P = 0.4514$). In particular, patients aged 60 years or above (715 out of 13,121) were not more infected (3 out of 715; 0.42%) than patients aged 60 years or below (88 out of 12,406 (0.71%); two-sided Fisher's exact test, $P = 0.4890$).

¹CIRI (Centre International de Recherche en Infectiologie), Université de Lyon, Université Claude Bernard Lyon 1, INSERM U1111, CNRS, UMR5308, ENS Lyon, Université Jean Monnet de Saint-Etienne, Lyon, France. ²Immunology laboratory, CIC1408, CHU Saint-Etienne, Saint-Etienne, France. ³Campus Vétérinaire de Lyon, VetAgro Sup, Université de Lyon, Marcy-l'Étoile, France. ⁴Occupational Health and Medicine Department, Hospices Civils de Lyon, Université Claude Bernard Lyon1, Iffsttar, UMRESTTE, UMR T_9405, Université de Lyon, Lyon, France. ⁵Joint Research Unit Civils Hospices de Lyon–bioMérieux, Hospices Civils de Lyon, Lyon Sud Hospital, Pierre-Bénite, France. ⁶Virology Laboratory, Institute of Infectious Agents, Laboratory Associated with the National Reference Centre for Respiratory Viruses, Hospices Civils de Lyon, Lyon, France. ⁷Centre de Recherche en Cancérologie de Lyon, INSERM U1052, CNRS UMR5286, Université de Lyon, Université Claude Bernard Lyon 1, Centre Léon Bérard, Lyon, France. ⁸These authors contributed equally: Bruno Pozzetto, Vincent Legros, Sophia Djebali, Véronique Barateau. ⁹These authors jointly supervised this work: François-Loïc Cosset, Stéphane Paul, Thierry Defrance, Jacqueline Marvel, Thierry Walzer, Sophie Trouillet-Assant. *A list of authors and their affiliations appears at the end of the paper. ✉e-mail: fcosset@ens-lyon.fr; stephane.paul@chu-st-etienne.fr; thierry.defrance@inserm.fr; jacqueline.marvel@inserm.fr; thierry.walzer@inserm.fr; sophie.assant@chu-lyon.fr

Table 1 | Infection rate in vaccinated HCWs at the Lyon University Hospital

Naive HCWs		BNT-BNT	ChAd-BNT
Vaccinated participants	Numbers of participants	10,609	2,512
	Median age (minimum–maximum)	42 (19–76) years ^a	33 (19–64) years ^a
SARS-CoV-2 RT-PCR positive at least 14 days after second vaccine dose	Numbers of infected participants (%)	81 (0.76) ^b	10 (0.4) ^b
	Median age (minimum–maximum)	41 (22–65) years	32 (22–49) years

^aTwo-sided Student's t-test, $P=5\times 10^{-24}$
^bLogistic regression model, $P=0.0384$

However, the vaccination regimen was significantly associated with the probability of being infected after vaccination ($P = 0.0384$). Individuals vaccinated with BNT-BNT were twice as likely to be infected than those vaccinated with ChAd-BNT (relative risk of 2.03).

Antibodies and virus neutralization

To understand the immunological basis of this difference, we assembled a cohort of healthcare workers (HCWs) without comorbidity (Covid-Ser-Vac). Half of this HCW cohort received the homologous BNT-BNT combination within the recommended 4-week interval between the two doses, whereas the second half received the BNT booster after receiving the first ChAd dose approximately 12 weeks before. For both groups, the mean age was 41 years and 34 years, respectively, and about 70% of participants were female (Table 2). Three blood samples were drawn: before vaccination, before the second dose and

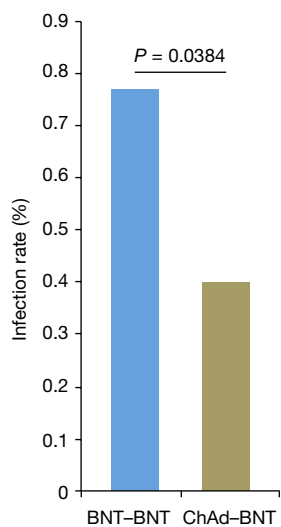


Fig. 1 | Incidence of SARS-CoV-2 infection after different vaccination regimens. Histograms show the infection rate (as documented by a positive SARS-CoV-2 RT-PCR result) among groups of HCWs who were vaccinated with the homologous BNT-BNT combination ($n = 81$ out of 10,609) within the recommended 4-week timeframe between the two doses or with the BNT booster after receiving the first ChAd dose ($n = 10$ out of 2,512) approximately 12 weeks before, as recorded by the service of occupational medicine, Hospices Civils de Lyon. Data show the infection rates that occurred 14 days after receiving booster up to the end of recording (15 August 2021). Statistical significance was calculated using a logistic regression model adjusted for age. Demographic data and other statistics are available in Table 1.

Table 2 | Clinical characteristics of patients in the Covid-Ser-Vac study

	Heterologous vaccine ($n=29$)	Homologous vaccine ($n=31$)	P value	Adjusted P value
Male sex (n (%))	9 (31.03)	8 (25.80)	0.7742	0.7742
Age in years (median (IQR))	34 (27–40)	41 (33–52)	0.0016	0.0056
Body mass index ¹ (n)	28	31		
Median (IQR)	22.25 (20.7–24.3)	23.12 (21.45–25.83)	0.2279	0.3988
Currently smoker (n (%))	5 (17.24)	8 (25.8)	0.5358	0.6251
Alcohol consumption ¹ (n (%))	7 (24.13)	5 (16.12)	0.5269	0.6251
Delay between two vaccine doses				
Median (IQR)	85 (84–85)	29 (26–31)	<0.0001	0.0007
Delay between second vaccine dose and third blood sample				
Median (IQR)	30 (28;34)	28 (27;31)	0.0245	0.057
Presence of comorbidity ^a (n (%))	0	0	NA	NA

Comorbidities include neurological disorders, cardiovascular disorders, hypertension, heart failure, diabetes, immune deficiency, liver disease, kidney disease, cancer, hypothyroid or rheumatic disease. For alcohol consumption, this was defined as consumption at least once a week. NA, not applicable. Mann-Whitney and Fisher two-sided tests were used for quantitative and qualitative variables (in italic), respectively. Adjusted P values were calculated using the Benjamini-Hochberg method.
^aIndicates one missing data.

4 weeks after the second dose. Immunological analyses were performed longitudinally (Extended Data Fig. 1), and a linear regression model was used to compare immune parameters between groups to adjust for age differences.

As previously shown^{6,7}, the BNT vaccine induced a stronger level of SARS-CoV-2 receptor binding domain (RBD) or spike S1-specific IgG than the ChAd vaccine after the first dose. However, these IgG titres were no longer statistically different between groups after the second dose (Fig. 2a, b). Moreover, the positivity rate was 100% for both heterologous and homologous vaccinations. Serum IgA levels measured after the booster vaccination tended to be greater in the homologous than in the heterologous setting (median (interquartile range (IQR)) of 46.7 ng m⁻¹ equivalent (Eq) (36.30–78.70 ng m⁻¹ Eq) versus 37.4 ng ml⁻¹ Eq (25.40–59.80 ng ml⁻¹ Eq), respectively; equivalence was to the standard used (Methods)) (Fig. 2c).

We then measured the ability of serum samples to neutralize SARS-CoV-2 spike-pseudotyped viral particles⁸. None of the sera displayed a detectable neutralizing activity before vaccination or after the first dose. However, most of the sera displayed a neutralizing activity after the second dose, and those from the ChAd-BNT vaccinated individuals displayed a higher neutralizing efficacy than those from the BNT-BNT vaccinated individuals (median (IQR) of 62% (34–93%) versus 99% (89–100%) of neutralization, respectively; $P < 0.001$) (Fig. 2d).

To validate these results, we tested the ability of the sera to prevent Vero E6 cell infection by SARS-CoV-2 isolates belonging to various clades, including 19A (B38 lineage), Alpha (B.1.1.7 lineage), Beta (B.1.351 lineage), Gamma (P1) and Delta (B.1.617.2 lineage)⁹. Each SARS-CoV-2 isolate was

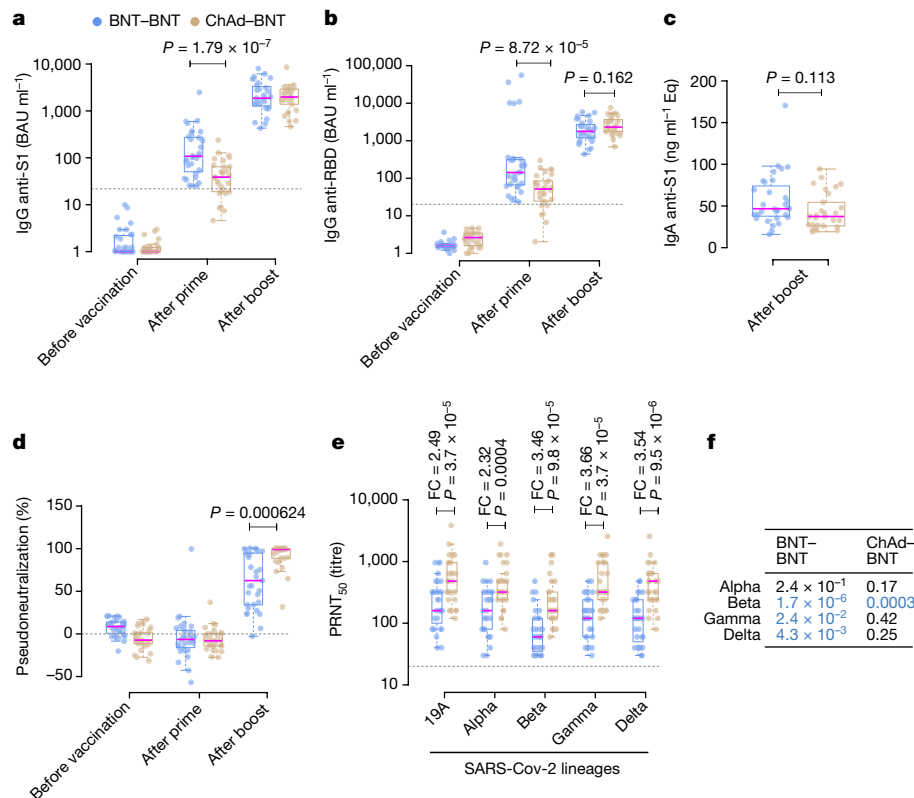


Fig. 2 | Heterologous vaccination induces higher neutralizing antibody titres.

a–c, Sera from ChAd-BNT ($n = 29$) or BNT-BNT ($n = 31$) individuals were assayed for S1-specific IgG (**a**), RBD-specific IgG (**b**) or S1-specific IgA (**c**) levels using commercial or custom-made ELISA tests at different times during the vaccination process as indicated (**a, b**) or 4 weeks after full vaccination (**c**). In **a–c**, concentrations are expressed in binding antibody units per ml (BAU ml^{-1}) or ng ml^{-1} Eq of immunoglobulin as indicated. Each serum sample was evaluated as a single measurement (**a, b**) or in triplicate (**c**). Dotted lines in **a** and **b** indicate positive detection according to the manufacturer. **d–f**, Sera from ChAd-BNT ($n = 29$) or BNT-BNT ($n = 31$) vaccinated individuals were assayed in triplicate for their capacity to neutralize the entry of virus-like particles pseudotyped with the Wuhan strain SARS-CoV-2 envelope (**d**) or in duplicate for their capacity to

neutralize infection of Vero E6 cells by different SARS-CoV-2 strains (**e, f**), as indicated. Data show the per cent of neutralization relative to a positive control (**d**) or the 50% plaque reduction neutralization test (PRNT_{50}) (**e**), and are expressed as dot plots, with one dot corresponding to one individual. The limit of detection is shown as a dotted line in **e**. FC, fold change in the mean of the indicated groups. In all panels, box-and-whiskers plots are shown (see Methods for details), and the median is represented by the magenta middle line. A linear regression model was used to compare values between groups, and this model was corrected for age. Exact P values are shown for the indicated comparisons when significant or nearly significant. **f**, Comparison of serum neutralizing activity against the reference lineage 19A and against the variants of concern for each group. P values are shown and calculated using the linear regression model described in **e**.

sequenced and confirmed to contain the characteristic mutations of its viral clade. The ChAd-BNT vaccinated individuals exhibited 2.3-fold to 3.6-fold higher serum neutralizing antibody titres against the different variants than BNT-BNT vaccinated individuals (Fig. 2e). Moreover, in the latter group, the neutralizing responses observed against the Beta, Gamma and Delta variants were significantly reduced compared with that against the 19A clade. By contrast, the neutralizing activity detected in sera from ChAd-BNT vaccinees was similarly high against all strains except the Beta clade (Fig. 2e, f). These data demonstrate that the neutralizing potential of antibodies generated by heterologous vaccination is less affected by spike mutations appearing in variants of concern than that of antibodies induced by homologous vaccination.

Vaccine-induced memory cells

We then studied the memory B cell (mBC) compartments using fluorescently labelled tetrameric RBDs to track RBD-specific mBCs and to analyse their phenotype (the gating analysis is presented in Extended Data Fig. 2a). As shown in Fig. 3a and Extended Data Fig. 2b, which correspond to concatenated flow cytometry plots, the frequency of RBD-binding mBCs was comparable for both vaccination groups after the prime dose but was on average twofold higher for the ChAd-BNT vaccination schedule after the booster dose. Moreover,

switched ($\text{IgD}^- \text{CD27}^+$) mBCs accounted for about 67% and 47% of the RBD-specific mBC pool in the ChAd-BNT group and the BNT-BNT group, respectively (Fig. 3b, c, Extended Data Fig. 2c). The expression pattern of IgM and IgG isotypes was next used to compare the immunoglobulin isotype distribution among the switched mBCs. The results showed that the homologous vaccination schedule promoted more IgG-switched mBCs (62% versus 48%) than the heterologous vaccination schedule (Fig. 3d, Extended Data Fig. 2d). Finally, to address the activation status of mBCs, we analysed their expression of CD21 and CD11c. It is generally considered that the concurrent loss of CD21 and the upregulation of CD11c are phenotypic features associated with B cell activation independent of the developmental stage¹⁰. Resting mBCs were therefore defined as $\text{CD21}^+ \text{CD11c}^-$ cells, whereas $\text{CD21}^- \text{CD11c}^+$, $\text{CD21}^+ \text{CD11c}^+$ and $\text{CD21}^- \text{CD11c}^-$ cells were globally considered as activated mBCs. The frequencies of activated RBD-specific mBCs were significantly enhanced in the ChAd-BNT group compared with the BNT-BNT group (Fig. 3e, Extended Data Fig. 2e). In particular, the proportions of the $\text{CD21}^- \text{CD11c}^+$ subset were almost three times higher in the ChAd-BNT group. Altogether, our results indicate that compared with the homologous vaccination schedule, the ChAd-BNT combination induces significantly more RBD-specific B cells, increases the frequencies of post-switch mBCs and induces a more active mBC generation process.

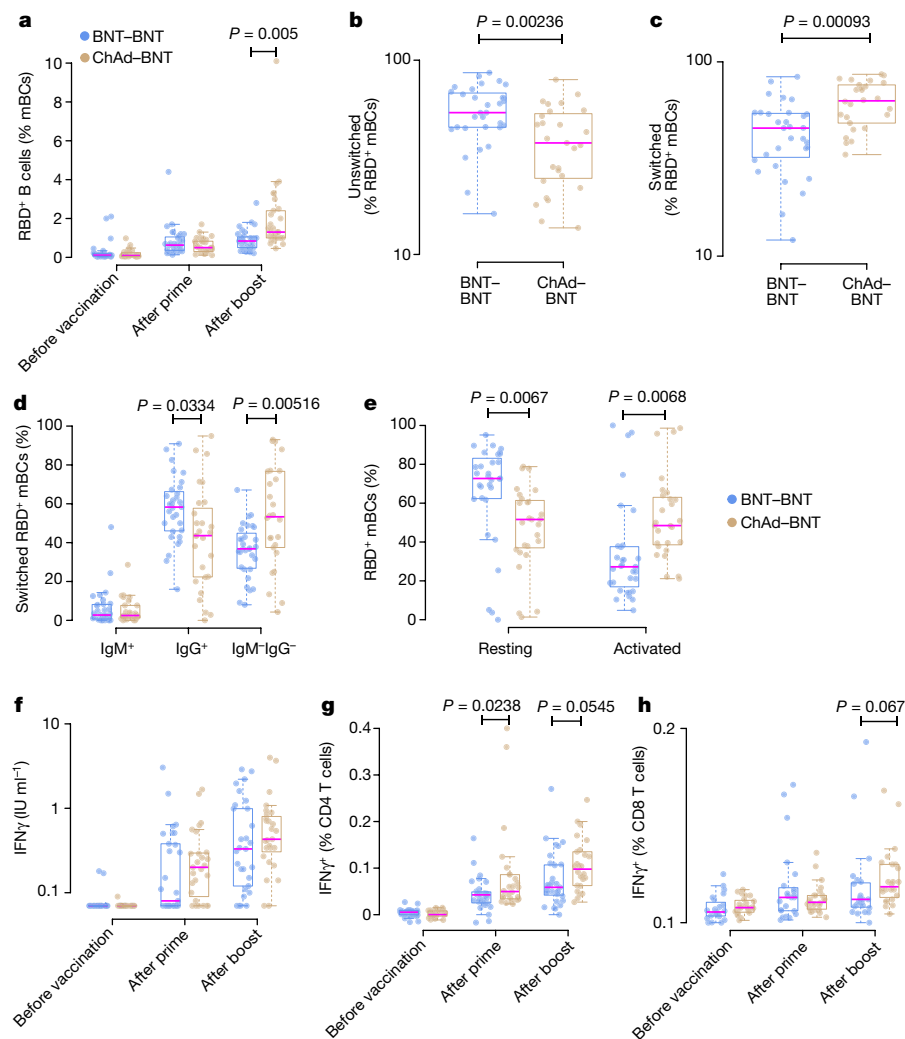


Fig. 3 | Analysis of RBD-specific memory B cells and spike-specific memory T cells in vaccinated individuals. a–e, Flow cytometry analyses of spike-specific mBCs. **a,** Frequencies of SARS-CoV-2 RBD-binding mBCs among the pool of polyclonal mBCs before vaccination, after prime and after boost injections. **b, c,** Proportions of unswitched (**b**) and switched (**c**) RBD-binding mBCs in per cent of RBD-binding mBCs. **d,** Pattern of immunoglobulin isotypes expressed by switched mBCs. **e,** Proportions of resting ($CD21^+CD11c^-$) and activated ($CD21^+CD11c^+$, $CD21^-CD11c^-$ and $CD21^-CD11c^+$) mBCs among the entire pool of RBD-binding mBCs. **f–h,** T cell responses. **f,** $IFN\gamma$ release after whole-blood stimulation with RBD peptides. $IFN\gamma$ was measured by ELISA in the supernatant. **g, h,** Flow cytometry analyses of the percentage of cells positive

for intracellular $IFN\gamma$ expression among CD4 (**g**) or CD8 (**h**) T cells after PBMC stimulation with commercial spike peptides. In all panels, box-and-whiskers plots (see Methods for details) of $n = 29$ and $n = 31$ participants in heterologous and homologous vaccination groups, respectively, are shown. The median value is shown in each group as a purple line. A high cellular mortality rate at the thawing step led to the exclusion of a few samples in each panel; each individual dot corresponds to one participant, and each measurement was performed once. In all panels, a linear regression model was used to compare values between groups, and this model was corrected for age. Exact P values are shown for the indicated comparisons when significant or nearly significant.

We then longitudinally monitored the T cell response of vaccinees against RBD peptides using a whole-blood interferon- γ ($IFN\gamma$) release assay. The T cell response was higher after ChAd immunization than after BNT priming and was similarly increased by the BNT booster dose in both groups (median of 0.33 UI ml^{-1} versus 0.43 UI ml^{-1}) (Fig. 3f). To confirm and consolidate these results, we measured the spike-specific CD4 and CD8 T cell response at the single-cell level by flow cytometry after stimulating peripheral blood mononuclear cells (PBMCs) from vaccinees with a pool of commercial peptides spanning the entire spike protein and then staining for intracellular $IFN\gamma$ (the gating strategy is presented in Extended Data Fig. 3). Both vaccination regimens were able to induce a progressive increase in the frequency of S-reactive CD4 and CD8 T cells from the pre-vaccine to the post-booster phase (Fig. 3g, h). However, the heterologous combination resulted in a stronger CD4 T cell response, both after priming and boosting, and in an increasing trend in the CD8 T cell response after the booster dose.

Finally, to understand interrelations between immune parameters, we performed a matrix analysis (Extended Data Fig. 4). This confirmed that the neutralizing antibody activity correlated with the titres of spike-specific IgG, regardless of the variant analysed, and not correlated with IgA levels. Moreover, the neutralization activity correlated with the percentage of switched RBD $^+$ mBCs and with the percentage of activated RBD $^+$ mBCs. This provides further support that better neutralizing antibodies are produced as a result of sustained B cell activation.

Discussion

Heterologous prime–boost vaccinations have been reported to be more immunogenic than homologous ones in experimental settings¹¹. This has also been proven for some human vaccines^{12,13}. Moreover, studies using mice have demonstrated the strong immunogenicity of the ChAd–BNT combination¹⁴. Here we report that heterologous ChAd–BNT vaccination

confers better protection against infection—which is associated with more switched mBCs and higher virus neutralizing antibody titres—irrespective of the variant analysed. This finding is of particular importance considering the global increase in the SARS-CoV-2 Delta variant¹⁵. Other studies reported better neutralizing potential of sera from ChAd-BNT vaccinated individuals compared with BNT-BNT vaccinated individuals, but these studies only used surrogate^{16,17} or pseudovirus¹⁸ neutralization assays. Moreover, the ability of such assays to predict neutralizing activity against authentic clinical virus isolates is still debated¹⁹.

Heterologous vaccination induced antibodies with a stronger neutralization potential than homologous vaccination, but the spike-specific IgG antibody titres were comparable. This result suggests that it is the quality of the antibodies that underlies the neutralization potential of the antibody response induced by heterologous vaccination. Assuming that the secondary antibody response is primarily derived from the mBC clones generated by primo-immunization, we can postulate that ChAd and BNT formulations elicit different mBC compartments. mBCs generated by the ChAd formulation could, for example, bear antigen receptors displaying a larger breadth of epitope recognition or a better fit for the SARS-CoV-2 spike protein. This could be linked to the different conformations of the spike protein, as that of the BNT vaccine bears a mutation stabilizing the protein in its pre-fusion conformation²⁰. Our data showed that mBCs still exhibit features of activation 4 weeks after the booster dose in the heterologous regimen, which suggests that the post-boost process of mBC differentiation is more active in this schedule. This could result from a more efficient or long-lasting germinal centre reaction that facilitates an extended cycle of somatic hypermutations and possibly output of B cell clones with higher affinity antigen receptors. An enlarged pool of CD4⁺ T helper cells could contribute to an amplified or prolonged germinal centre reaction. In keeping with this notion, we report here a higher frequency of spike-specific CD4 T cells after priming with the ChAd vaccine, which has been observed in other studies^{6,7}. Moreover, stronger T cell responses may contribute to better protection independently of B cell responses²¹.

The better neutralization potential of sera from ChAd-BNT vaccinated individuals could also be linked to their relatively lower level of SI-specific IgA levels. Indeed, plasma IgA monomers specific to SARS-CoV-2 proteins are twofold less potent than IgG equivalents²². Furthermore, IgA levels persist better than IgG after infection, which coincides with a reduction in the serum neutralizing potential²³. Following a possible competition between serum IgA and IgG, the decrease in IgA levels in heterologous vaccination conditions may lead to better neutralization effects. This phenomenon has already been observed in the context of the RV144 vaccination trial against HIV-1, in which the level of envelope-specific IgA correlated with the risk of infection²⁴. In this context, IgA was also found to inhibit antibody-dependent cell cytotoxicity by competing with IgG²⁵.

Our data do not allow the discarding of the possibility that the later timing of administration of the booster dose contributed to the high efficacy of the heterologous regimen. Still, it is noteworthy that the size of the RBD⁺ mBC pool after the prime dose was comparable for both groups of vaccinees, despite the disparity in the analysis time point after the prime vaccination (4 versus 12 weeks). This observation indicates that the extended interval between prime and boost in the ChAd-BNT cohort has not been translated into a greater size of the RBD-specific mBC compartment. It has been recently demonstrated for both the ChAd vaccine²⁶ and the BNT vaccine²⁷ that long injection time intervals (12 weeks or more) provide higher binding and neutralizing antibody titres than shorter intervals (less than 6 weeks). For a comparable long vaccination interval (more than 9 weeks), the heterologous ChAd-BNT vaccination schedule induced better humoral immunity (titres and neutralization) than the homologous ChAd-ChAd combination²⁸. To our knowledge, there is only one study in which ChAd-BNT and BNT-BNT vaccination schedules were compared with the same prime-boost interval (4 weeks)⁶. That study⁶

concluded that for short intervals, the humoral responses induced by both regimens were comparable. However, a longer interval (that is, 12 weeks) between prime and boost could be needed to allow the synergy between heterologous vaccines.

Together, we present a real-world observational study of HCWs showing that the heterologous ChAd-BNT vaccination regimen confers stronger protective immunity than the homologous BNT-BNT prime-boost schedule. As hidden confounding factors might be present in our study (for example, different levels of exposure to the virus), confirmatory studies and a longer follow-up of vaccinated participants are warranted. However, our data suggest that the heterologous combination could be particularly suitable for immunocompromised individuals.

Online content

Any methods, additional references, Nature Research reporting summaries, source data, extended data, supplementary information, acknowledgements, peer review information; details of author contributions and competing interests; and statements of data and code availability are available at <https://doi.org/10.1038/s41586-021-04120-y>.

1. Greinacher, A. et al. Thrombotic thrombocytopenia after ChAdOx1 nCoV-19 vaccination. *N. Engl. J. Med.* **384**, 2092–2101 (2021).
2. Scully, M. et al. Pathologic antibodies to platelet factor 4 after ChAdOx1 nCoV-19 vaccination. *N. Engl. J. Med.* **384**, 2202–2211 (2021).
3. Polack, F. P. et al. Safety and efficacy of the BNT162b2 mRNA Covid-19 vaccine. *N. Engl. J. Med.* **383**, 2603–2615 (2020).
4. Ramasamy, M. N. et al. Safety and immunogenicity of ChAdOx1 nCoV-19 vaccine administered in a prime-boost regimen in young and old adults (COV002): a single-blind, randomised, controlled, phase 2/3 trial. *Lancet* **396**, 1979–1993 (2021).
5. Voysey, M. et al. Safety and efficacy of the ChAdOx1 nCoV-19 vaccine (AZD1222) against SARS-CoV-2: an interim analysis of four randomised controlled trials in Brazil, South Africa, and the UK. *Lancet* **397**, 99–111 (2021).
6. Liu, X. et al. Safety and immunogenicity of heterologous versus homologous prime-boost schedules with an adenoviral vectored and mRNA COVID-19 vaccine (Com-COV): a single-blind, randomised, non-inferiority trial. *Lancet* **398**, 856–869 (2021).
7. Hillus, D. et al. Safety, reactogenicity, and immunogenicity of homologous and heterologous prime-boost immunisation with ChAdOx1 nCoV-19 and BNT162b2: a prospective cohort study. *Lancet Respir. Med.* **9**, 1255–1265 (2021).
8. Legros, V. et al. A longitudinal study of SARS-CoV-2-infected patients reveals a high correlation between neutralizing antibodies and COVID-19 severity. *Cell. Mol. Immunol.* **18**, 318–327 (2021).
9. Gonzalez, C. et al. Live virus neutralisation testing in convalescent patients and subjects vaccinated against 19A, 20B, 20I/501Y.V1 and 20H/501Y.V2 isolates of SARS-CoV-2. *Emerg. Microbes Infect.* **10**, 1499–1502 (2021).
10. Sanz, I. et al. Challenges and opportunities for consistent classification of human B cell and plasma cell populations. *Front. Immunol.* **10**, 2458 (2019).
11. Lu, S. Heterologous prime-boost vaccination. *Curr. Opin. Immunol.* **21**, 346–351 (2009).
12. Jou, J., Harrington, K. J., Zocca, M.-B., Ehrnrooth, E. & Cohen, E. E. W. The changing landscape of therapeutic cancer vaccines—novel platforms and neoantigen identification. *Clin. Cancer Res.* **27**, 689–703 (2021).
13. Levine, M. Z. et al. Heterologous prime-boost with A(H5N1) pandemic influenza vaccines induces broader cross-clade antibody responses than homologous prime-boost. *NPJ Vaccines* **4**, 22 (2019).
14. Spencer, A. J. et al. Heterologous vaccination regimens with self-amplifying RNA and adenoviral COVID vaccines induce robust immune responses in mice. *Nat. Commun.* **12**, 2893 (2021).
15. Alizon, S. et al. Rapid spread of the SARS-CoV-2 Delta variant in some French regions, June 2021. *Euro Surveill.* **26**, 2100573 (2021).
16. Schmidt, T. et al. Immunogenicity and reactogenicity of heterologous ChAdOx1 nCoV-19 mRNA vaccination. *Nat. Med.* **27**, 1530–1535 (2021).
17. Tenbusch, M. et al. Heterologous prime-boost vaccination with ChAdOx1 nCoV-19 and BNT162b2. *Lancet Infect. Dis.* **21**, 1212–1213 (2021).
18. Groß, R. et al. Heterologous ChAdOx1 nCoV-19 and BNT162b2 prime-boost vaccination elicits potent neutralizing antibody responses and T cell reactivity. Preprint at <https://doi.org/10.1101/2021.05.30.21257971> (2021).
19. von Rhein, C. et al. Comparison of potency assays to assess SARS-CoV-2 neutralizing antibody capacity in COVID-19 convalescent plasma. *J. Virol. Methods* **288**, 114031 (2021).
20. Juraszek, J. et al. Stabilizing the closed SARS-CoV-2 spike trimer. *Nat. Commun.* **12**, 244 (2021).
21. Sette, A. & Crotty, S. Adaptive immunity to SARS-CoV-2 and COVID-19. *Cell* **184**, 861–880 (2021).
22. Wang, Z. et al. Enhanced SARS-CoV-2 neutralization by dimeric IgA. *Sci. Transl. Med.* **13**, eabf1555 (2021).
23. Wang, Z. et al. Naturally enhanced neutralizing breadth against SARS-CoV-2 one year after infection. *Nature* **595**, 426–431 (2021).
24. Haynes, B. F. et al. Immune-correlates analysis of an HIV-1 vaccine efficacy trial. *N. Engl. J. Med.* **366**, 1275–1286 (2012).

25. Tomaras, G. D. et al. Vaccine-induced plasma IgA specific for the C1 region of the HIV-1 envelope blocks binding and effector function of IgG. *Proc. Natl Acad. Sci. USA* **110**, 9019–9024 (2013).
26. Voysey, M. et al. Single-dose administration and the influence of the timing of the booster dose on immunogenicity and efficacy of ChAdOx1 nCoV-19 (AZD1222) vaccine: a pooled analysis of four randomised trials. *Lancet* **397**, 881–891 (2021).
27. Payne, R. P. et al. Immunogenicity of standard and extended dosing intervals of BNT162b2 mRNA vaccine. *Cell* **184**, 5699–5714 (2021).
28. Barros-Martins, J. et al. Immune responses against SARS-CoV-2 variants after heterologous and homologous ChAdOx1 nCoV-19/BNT162b2 vaccination. *Nat. Med.* **27**, 1525–1529 (2021).

Publisher's note Springer Nature remains neutral with regard to jurisdictional claims in published maps and institutional affiliations.

© The Author(s), under exclusive licence to Springer Nature Limited 2021

Covid-Ser study group

Kahina Saker⁵, Christelle Compagnon⁵, Bouchra Mokdad⁵, Constance d'Aubarede⁴, Virginie Pitiot⁴, Vanessa Escuret^{1,6}, Florence Morfin^{1,6}, Mary-Anne Traubaud⁶, Margaux Prieux¹, Valérie Dubois¹, Laurence Josset^{1,6} & Soizic Daniel⁵

Methods

Ethical statement and cohort description

The use and analysis of data from the occupational health medical file were authorized after a regulatory declaration to the National Commission for Information Technology and Civil Liberties according to the reference methodology (declaration MR004 number 20-121 of 30 April 2020). The declaration of SARS-CoV-2 infection is compulsory for all staff to obtain daily allowances without loss of salary during the imposed quarantine.

For the Covid-Ser-Vac study, clinical data were recorded by a trained clinical research associate using Clinsight software (v.Csonline 7.5.720.1). Blood samples were processed and stored at the Centre de Ressource Biologique Neurobiotec, 69500 Bron. Sixty naive HCWs for COVID-19 and vaccinated with BNT and/or ChAd vaccines were included in a prospective longitudinal cohort study conducted at the Hospices Civils de Lyon. Blood sampling was performed before vaccination, before the second dose of vaccine and 4 weeks after the end of vaccination schedule. The absence of previous SARS-CoV-2 infection was confirmed using the Wantai SARS-CoV-2 Ab total assay in the pre-vaccine sample. Demographic characteristics and delays between doses are depicted in Table 2 and Extended Data Fig. 1. Written informed consent was obtained from all participants. Ethics approval was obtained from the national review board for biomedical research in April 2020 (Comité de Protection des Personnes Sud Méditerranée I, Marseille, France; ID RCB 2020-A00932-37), and the study was registered at ClinicalTrials.gov (NCT04341142).

Measurement of IgG titres

Sera were immediately stored at -80°C after blood sampling. S1-specific IgG and RBD-specific IgG were measured using Siemens Atellica IMSARS-CoV-2 IgG (sCOVG) and bioMérieux Vidas SARS-CoV-2 IgG diagnosis kits, respectively, according to the manufacturers' recommendations. For standardization of these assays to the first World Health Organization international standard, the concentrations were transformed into binding antibody units per ml (BAU ml^{-1}) using the conversion factors provided by the manufacturers.

Measurement of spike-specific IgA

ELISAs to evaluate IgA binding to the SARS-CoV-2 spike protein were performed as previously described²⁹. High-binding 96-half-well plates (2310M, Nunc) were coated with 100 μl per well of a spike protein solution ($1\ \mu\text{g ml}^{-1}$; 40591-V08H spike S1-RBD, Sino Biologicals) in PBS overnight at 4°C . Plates were washed with washing buffer containing 1 \times PBS with 0.05% Tween 20 (Sigma-Aldrich) and incubated with 170 μl of blocking buffer per well containing 1 \times PBS with 3% fat milk powder and 0.05% Tween 20 (Sigma-Aldrich) for 1 h at room temperature. Immediately after blocking, recombinant anti-RBD IgA (B Cell Design, IB3C4 PV) or serum samples diluted in PBS were added and incubated for 1 h at 37°C . Plasma samples were assayed at a 1:100 starting dilution and 7 additional 3-fold serial dilutions. Recombinant human anti-RBD IgA was used to perform a calibration curve starting at $1.5\ \mu\text{g ml}^{-1}$. Plates were washed and then incubated with anti-human IgA (A0295, Sigma-Aldrich) secondary antibody conjugated to horseradish peroxidase in blocking buffer at 1:10,000. Plates were developed by the addition of the horseradish peroxidase substrate 3,3',5,5'-tetramethylbenzidine (TMB; 34021, Thermo Fisher Scientific) for 10 min, and the developing reaction was stopped by adding 50 μl of 1 M HCl. Optical density units were measured at 450 nm in a microplate reader (Tecan). For serum samples, a positive control (serum pool from critically ill patients with COVID-19, diluted 200-fold in PBS) and a negative control (pool of historical serum samples) were added in duplicate to each run. After deduction of the background, a relative content in IgA equivalent ($\text{ng ml}^{-1}\text{Eq}$) was calculated using the calibration curve. The limit of detection of the assay was $0.1\ \text{ng ml}^{-1}\text{Eq}$.

Live-virus neutralization experiments

A plaque reduction neutralization test (PRNT) was used for the detection and titration of neutralizing antibodies. A tenfold dilution of each serum specimen in culture medium was first heated for 30 min at 56°C to avoid complement-linked reduction of viral activity. Serial twofold dilutions (tested in duplicate) of the serum specimens in culture medium were mixed in equal volume with the live SARS-CoV-2 virus. After gentle shaking and a contact of 30 min at room temperature in plastic microplates, 150 μl of the mix was transferred into 96-well microplates covered with Vero E6 cells (American Type Culture Collection (ATCC), CRL-1586, not authenticated but regularly tested for mycoplasma contamination). The plates were incubated at 37°C in a 5% CO_2 atmosphere. Infection efficiency was evaluated by microscopy 5 days later when the cytopathic effect of the virus control reached 100–500 TCID_{50} (median culture infectious dose) per 150 μl . Neutralization was recorded if more than 50% of the cells present in the well were preserved. The neutralizing titre was expressed as the inverse of the higher serum dilution that exhibited neutralizing activity; a threshold of 20 was used ($\text{PRNT}_{50}\text{ titre} \geq 20$). All experiments were performed in a biosafety level 3 laboratory. The different viral strains that were used were sequenced and deposited at GISAID (<https://www.gisaid.org/>) (accession numbers EPI_ISL_1707038 19A (B.38 lineage); EPI_ISL_1707039 Alpha (B.1.1.7 lineage); EPI_ISL_768828 Beta (B.1.351 lineage); EPI_ISL_1359892 Gamma (P.1 lineage); and EPI_ISL_1904989 Delta (B.1.617.2 lineage)).

Monitoring of T cell responses using whole-blood IFN γ release assay

Fresh blood collected in heparinized tubes was stimulated for 22 h at 37°C under 5% CO_2 with SARS-CoV-2 peptide pools (derived from the prototype Wuhan strain NC_045512.2) targeting RBD (46 peptides, $[\text{C}] = 8\ \mu\text{g ml}^{-1}$) (bioMérieux) diluted in IGRA solution (bioMérieux). The peptides (15-mer) encompassed the entire protein sequence and overlapped by five residues. The IGRA solution was used as a negative control and a mitogen as a positive control. The concentration of IFN γ in the supernatant was measured using a VIDAS automated platform (VIDAS IFN γ RUO, bioMérieux). The measuring range was 0.08–8 IU ml^{-1} and WB IGRA positivity thresholds were defined at $0.08\ \text{IU ml}^{-1}$. The IFN γ response was defined as detectable when the IFN γ concentration of the test was above threshold and the negative control was below threshold or when the IFN γ concentration of the test minus IFN γ concentration of the negative control was above threshold.

Monitoring of T cell responses by flow cytometry

Overnight-rested PBMCs were stimulated with SARS-CoV-2 overlapping peptide pools against SARS-CoV-2 spike protein (PepTivator, Miltenyi Biotec) at a final concentration of $1\ \mu\text{g ml}^{-1}$ for 1 h in the presence of $1\ \mu\text{g ml}^{-1}$ monoclonal antibodies CD28 and CD49d, and then for an additional 5 h with GolgiPlug and GolgiStop (BD Biosciences). Dead cells were labelled using Fixable Viability eFluor 780 dye (Thermo Fisher Scientific). Surface markers were stained using BV786-conjugated anti-CD3 (BD Biosciences, 565491; diluted 1:100), BUV486-conjugated anti-CD4 (BD Biosciences, 612937; 1:50), PE-Cy7-conjugated anti-CD8 (BioLegend, 301012; 1:100), APC-Cy7-conjugated anti-CD14 (BioLegend, 301820; 1:100), APC-Cy7-conjugated anti-CD56 (BioLegend, 362512; 1:100) and APC-Cy7-conjugated anti-CD19 (BioLegend, 302218; 1:100). Cells were then washed, fixed with Cytofix/Cytoperm (BD Biosciences) and stained with PE-conjugated anti-IFN γ (BioLegend). Negative controls without peptide stimulation were run for each sample. All results were acquired on a BD LSRFortessa (BD Biosciences) flow cytometer using the BD FACSDIVA v.8.01 software and analysed using FlowJo v.10.6.1 software.

SARS-CoV-2 pseudoparticle preparation and neutralization

SARS-CoV-2 spike-pseudotyped murine leukaemia virus retrovirus particles were produced as described for SARS-CoV³⁰. In brief, HEK293T

Article

cells (ATCC, CRL-1573, not authenticated but regularly tested for mycoplasma contamination) were transfected with constructs expressing murine leukaemia virus Gag-Pol, the green fluorescent protein (GFP) reporter and the SARS-CoV-2 spike protein (a gift from D. Lavillette (CAS Key Laboratory of Molecular Virology & Immunology, Institut Pasteur of Shanghai Chinese Academy of Sciences, Pasteur College, Soochow University, Jiangsu, China)). Control particles pseudotyped with the unrelated RD114 virus surface glycoprotein (from a cat endogenous virus) were generated as previously described³¹. For neutralization assays, a sample of approximately 1×10^3 pseudoparticles was incubated with a 100-fold dilution of sera or control antibodies for 1 h at 37 °C, spinoculated for 2 h at 2,500g before infection of Vero E6 cells. After 72 h of infection, the percentage of GFP-positive cells was determined by flow cytometry. As a control, the same procedure was performed using RD114 pseudoparticles. Anti-spike SARS-CoV-2 RBD (Sino Biological, 40150-V08B2) and anti-gp70 RD114 (ViroMed Biosafety Labs) antibodies were used with a 100-fold dilution as positive and negative control, respectively.

Generation of fluorescent SARS-CoV-2 RBD tetramers

Biotinylated recombinant RBD domain of SARS-CoV-2 RBD was purchased from Miltenyi Biotech (130-127-457) and tetramerized with either streptavidin-PE (Becton Dickinson (BD)) or with streptavidin-APC (BioLegend, 105243).

Flow cytometry analysis of SARS-CoV-2 RBD-specific B cells

Cryopreserved PBMCs were centrifuged and suspended in PEB buffer (PBS with 0.5% BSA and 2 mM EDTA) and incubated with Fc receptor block (Miltenyi, 130-059-901) for 15 min at 4 °C (dilution 1:10). Next, cells were washed in PEB and stained for 30 min in brilliant stain buffer at 4 °C in the dark using the following antibodies together with both the PE- and APC-conjugated recombinant RBD tetramers: anti-CD3-APC Fire 810 (BioLegend, 344858; diluted 1:100); anti-CD11c-BV785 (BioLegend, 301644; 1:50); anti-CD19-PE Vio770 (Miltenyi, 130-113-170; 1:100); anti-CD20-BV421 (BD, 562873; 1:100); anti-CD21-BUV496 (BD, 750614; 1:50); anti-CD27-PercP-Vio700 (Miltenyi, 130-113-632; 1:100); anti-CD38-Viobright FITC (Miltenyi, 130-113-433; 1:50); anti-IgM-PE-CF594 (BD, 562539; 1:50); anti-IgD-BV605 (BioLegend, 348232; 1:50); and anti-IgG-BV480 (BD, 746341; 1:50). Cells were washed in PEB and resuspended in a PEB dilution (1:500) of the fixable viability dye eFluor 780 (eBiosciences, 65-0865-18). They were next washed and fixed with 4% paraformaldehyde for 20 min at 4 °C in the dark before a final wash and resuspension for analysis. Cells were then acquired on a Cytek Aurora spectral flow cytometer equipped with five lasers operating at 355 nm, 405 nm, 488 nm, 561 nm and 640 nm using the SpectroFlo V.2.2.0 (Cytek) software. Data were analysed using FlowJo 10.6.1 software (BD).

Statistical analyses

Statistical modelling for epidemiological data. To model the probability of being infected knowing the subject age and the used vaccination regimen, we used the generalized linear model (glm) function in R to perform a multiple logistic regression model with the logit link function. The outcome variable was the infection status, whereby infected = 1 and not infected = 0. Our predictors were the age, as a continuous variable (considered as a possible confounder), and the vaccination regimen, whereby Chad-BNT = 0 and BNT-BNT = 1. On the basis of the model coefficients for the vaccination regimen ($B_0 = -5.306$ and $B_1 = 0.712$), we also assessed the relative risk (RR) as follows: $RR = (1 + \exp(-B_0)) / (1 + \exp(-B_0 - B_1))$.

Statistical analysis for immunological and virological analyses.

ChAd-BNT and BNT-BNT populations showed a significant difference in the average ages. To test for the consequence of the vaccination regimen on the different immune parameters, we fitted a multiple linear regression model, which allows for the correction of age (as a possible confounding factor) by including age and vaccination regimen simultaneously as predictors in the right explanatory side of the lm function in R (one model per immune parameter). Results of statistical significance displayed in Figs. 2 and 3 are from these adjusted models, for which age showed no effect. For box and whiskers plots, the upper and lower bounds of the box are the 75th and the 25th percentile (the third Q3 and first Q1 quartile), respectively. The IQR = $Q_3 - Q_1$; an observation was considered an outlier if it was above $Q_3 + 1.5 \times IQR$ or below $Q_1 - 1.5 \times IQR$. Upper and lower whiskers represent the maximum and the minimum values, respectively, without taking into account the outliers.

Reporting summary

Further information on research design is available in the Nature Research Reporting Summary linked to this paper.

Data availability

Viral sequences are available at GISAID (accession numbers EPI_ISL_1707038 19A (B.38 lineage); EPI_ISL_1707039 Alpha (B.1.1.7 lineage); EPI_ISL_768828 Beta (B.1.351 lineage); EPI_ISL_1359892 Gamma (P.1 lineage); and EPI_ISL_1904989 Delta (B.1.617.2 lineage)). Source data are provided with this paper.

29. Amanat, F. et al. A serological assay to detect SARS-CoV-2 seroconversion in humans. *Nat. Med.* **26**, 1033–1036 (2020).
30. Broer, R., Bosen, B., Spaan, W., Cosset, F.-L. & Corver, J. Important role for the transmembrane domain of severe acute respiratory syndrome coronavirus spike protein during entry. *J. Virol.* **80**, 1302–1310 (2006).
31. Lavillette, D. et al. Human serum facilitates hepatitis C virus infection, and neutralizing responses inversely correlate with viral replication kinetics at the acute phase of hepatitis C virus infection. *J. Virol.* **79**, 6023–6034 (2005).

Acknowledgements This study was supported by IDEX Lyon (HPI-2019), operated by the French National Research Agency (ANR-11-IDEX-0007), INSERM-Transfert and by institutional grants from Fondation des Hospices Civils de Lyon, INSERM, CNRS, UCBL1 and ENS de Lyon. We thank the following staff members and individuals: all the staff members of the Occupational Health and Medicine Department of the Hospices Civils de Lyon (who contributed to the sample collection) and all the clinical research associates for their excellent work; the staff members of SFR Biosciences (UAR3444/CNRS, US8/INSERM, ENS de Lyon, UCBL) AnIRA-cytometry, E. Devèvre, S. Dussurgey and V. Malassigné; K. Brahima and all the members of the clinical research and innovation department for their reactivity (DRCI, Hospices Civils de Lyon); and all the HCWs for their participation in this clinical study. Human biological samples and associated data were obtained from NeuroBioTec (CRB HCL, Lyon France, Biobank BB-0033-00046).

Author contributions B.P., V.L., S. Djebali, V.B., M. Villard, L.P., M.Y.-N., S. Denolly, B.B., T.B., M. Valette, A.B. and K.B.-P. performed experiments and analysed the data. T.A. helped with the analysis of flow cytometry data and O.A. performed statistical analyses. N.G., J.-B.F. and A.M.-P. analysed the clinical infection data. The Covid-Ser study members collected the samples and performed experiments. B.L. supervised some of the experimental tasks. F.-L.C., S.P., T.D., J.M., T.W. and S.T.-A. designed the study, analysed the data and wrote the manuscript.

Competing interests K.B.-P. is a bioMérieux employee.

Additional information

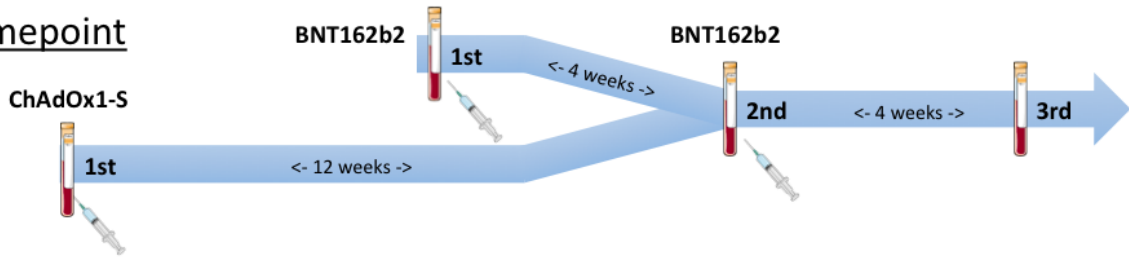
Supplementary information The online version contains supplementary material available at <https://doi.org/10.1038/s41586-021-04120-y>.

Correspondence and requests for materials should be addressed to François-Louis Cosset, Stéphane Paul, Thierry DeFrance, Jacqueline Marvel, Thierry Walzer or Sophie Trouillet-Assant.

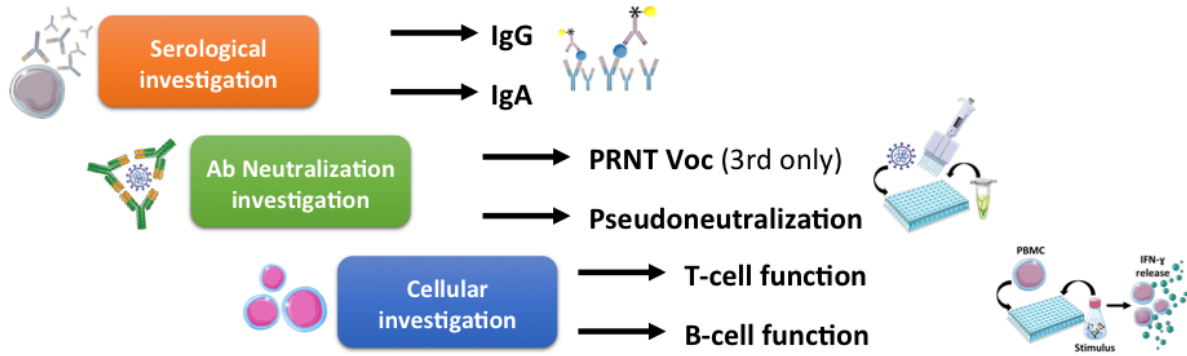
Peer review information Nature thanks Yunda Huang, Pei-Yong Shi and the other, anonymous, reviewer(s) for their contribution to the peer review of this work. Peer reviewer reports are available.

Reprints and permissions information is available at <http://www.nature.com/reprints>.

Timepoint

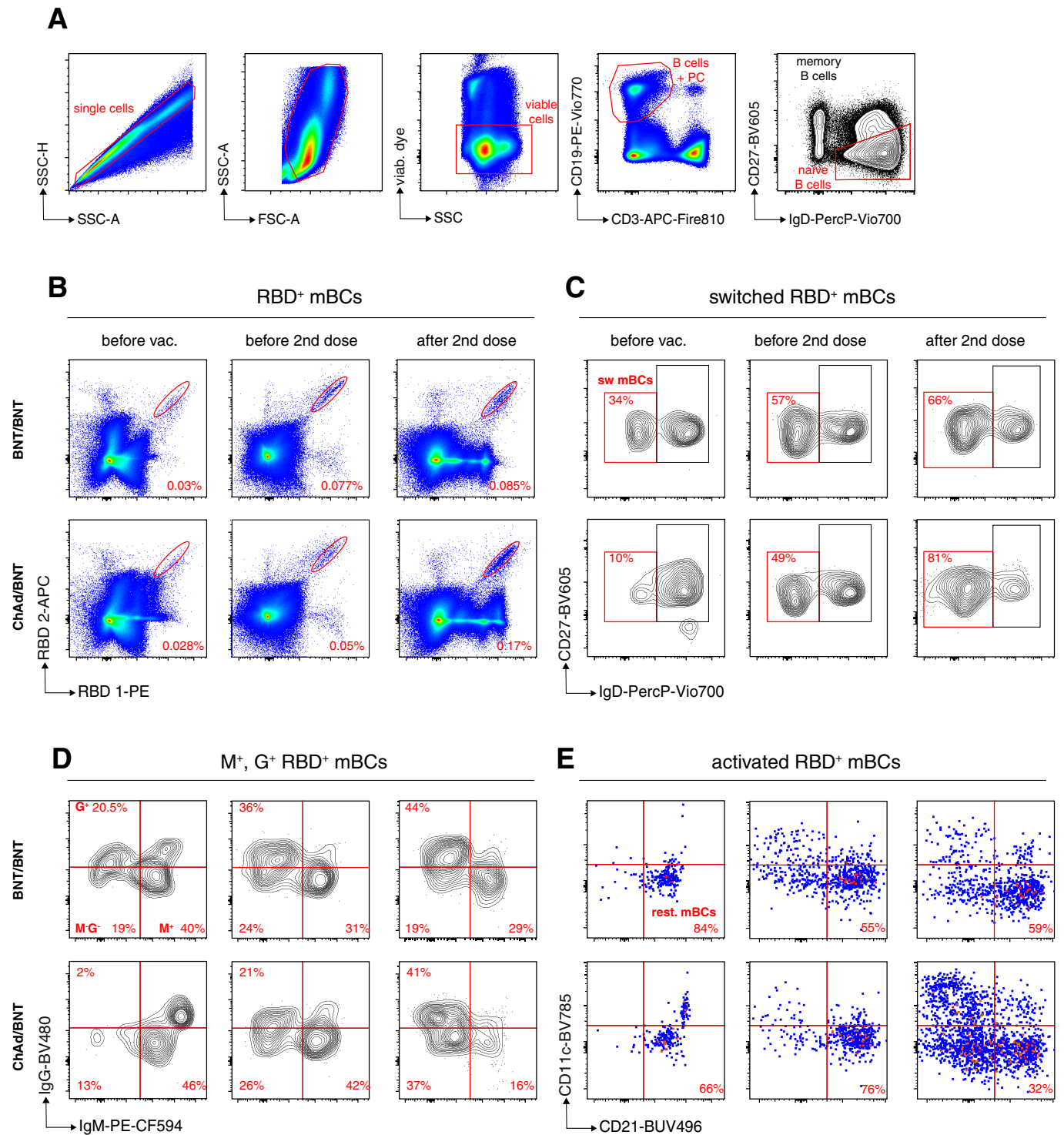


Experimental set-up



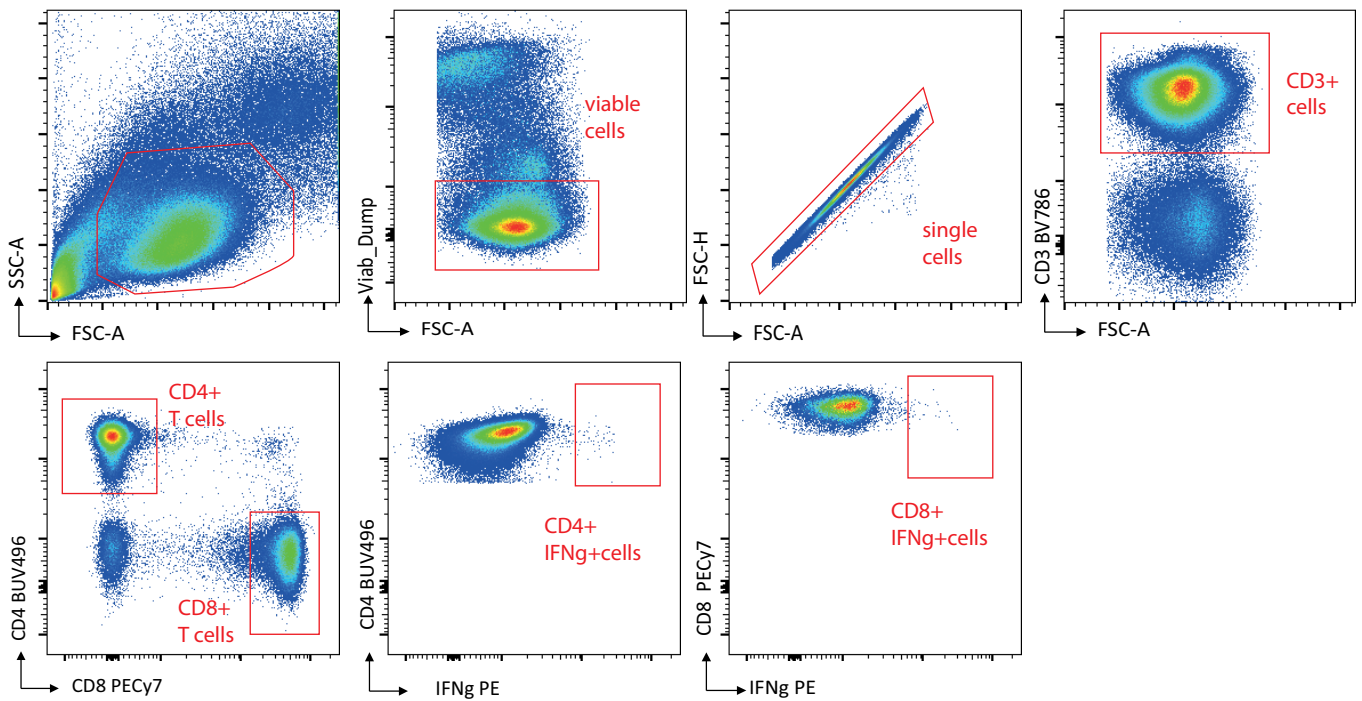
Extended Data Fig. 1 | Study design. Sixty HCWs naïve for COVID-19 and vaccinated with the Pfizer ChAd/BNT or the BNT/BNT combination were included in a prospective longitudinal cohort study. Blood sampling was performed as described, before vaccination, before the second dose of vaccine and 4 weeks after the end of vaccination schedule. Different immunological analyses were performed on the blood samples, including serological investigations (Spike-specific IgA and IgG), serum neutralization assays (both

plaque reduction neutralization test (PRNT) and pseudoneutralization), analysis of Spike-specific T cells and RBD-specific memory B cells, at various time points indicated in the text. Parts of the figure were drawn by using pictures from Servier Medical Art (<http://smart.servier.com/>), licensed under a Creative Commons Attribution 3.0 Unported License (<https://creativecommons.org/licenses/by/3.0/>).



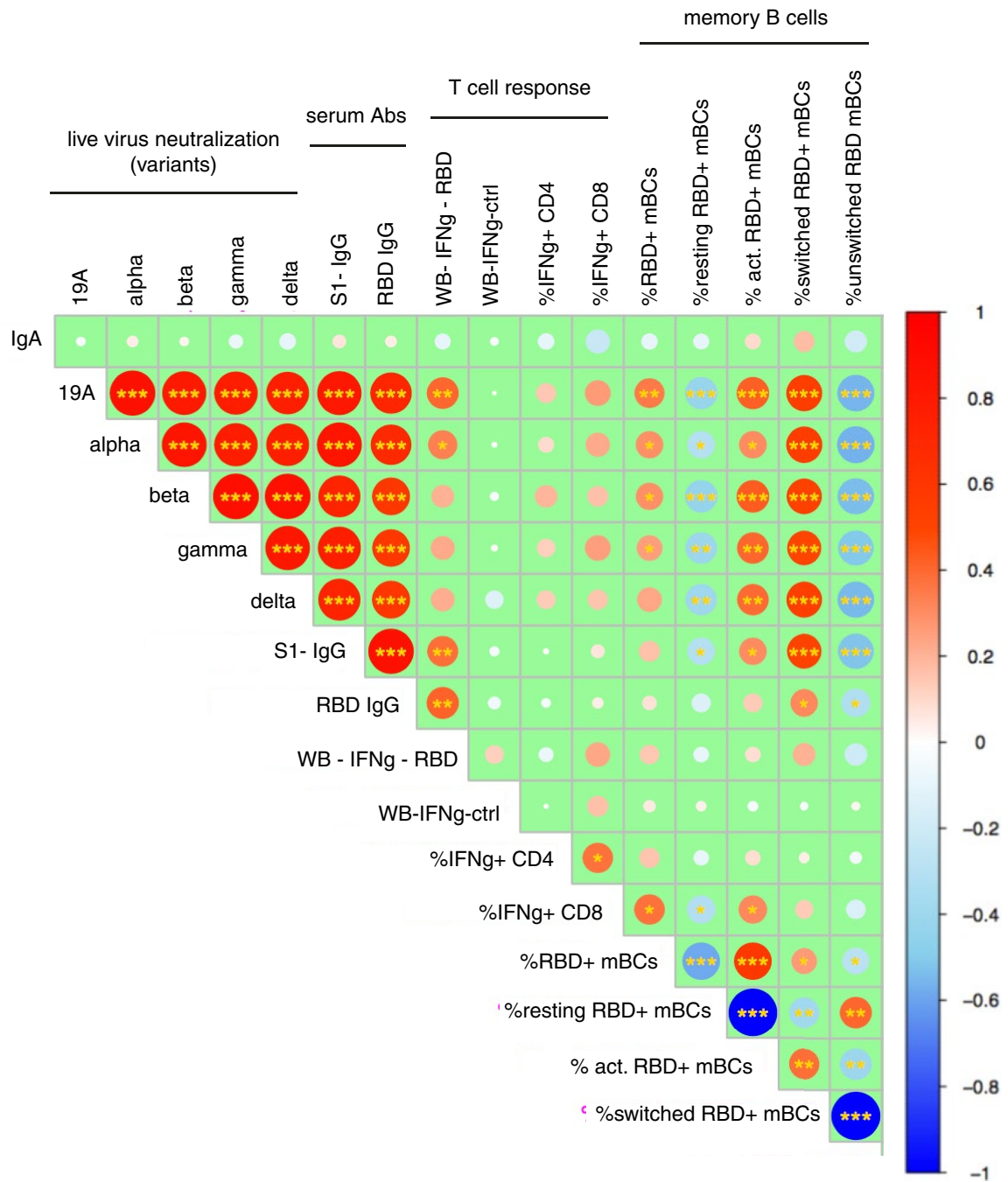
Extended Data Fig. 2 | Analysis of RBD-specific memory B cells. (A) Gating strategy. From left to right, the first three pseudo-color plots show the successive gates applied for single cells and viable cells. B cells were gated as CD19⁺/CD3⁺ cells (4th plot). Within the B cell gate, memory B cells (mBCs) were defined as non-naïve B cells on the same biparameter plot (5th plot). (B-E) Concatenated phenotypic profiles of RBD-specific mBCs for all individuals in the ChAd/BNT and BNT/BNT groups at three time points (before vaccination, before the 2nd dose, after the second dose). For each group, the phenotypic profiles correspond to the concatenation of the FACS analysis data collected

from 30 individual vaccinees. (B) Visualization of RBD-binding B cells in the mBC gate. (C) Visualization of the proportion of switched (IgD⁺) and unswitched (IgD⁻) B cells among the RBD-specific mBC pool. (D) Visualization of the pattern of Ig isotype expression by RBD-specific mBCs. (E) Visualization of the distribution of RBD-binding B cells within the resting (CD21⁺CD11c⁻) and “activated” (CD21⁻CD11c⁺) mBC compartments. The mean frequencies of RBD-specific mBCs falling into each quadrant are indicated in red.



Extended Data Fig. 3 | Analysis of SARS-CoV-2-specific T cells. PBMCs were stimulated as detailed in the methods and stained for CD3, CD4, CD8, CD14, CD56 and CD19 expression and with a dead cell marker. Cells were gated from left to right and top to bottom. The Viab/dump channel includes antibodies

against CD14, CD19, CD56 and a viability marker. The frequency of CD4 or CD8 T cells positive for intracellular IFNg was measured as shown in the central and right bottom panels.



Extended Data Fig. 4 | Analysis of inter-relationships between immune parameters. A matrix file with all immunological measurements for all vaccinated individuals showing the Spearman correlations and associated

p-values. The size and the color of the circles correspond to the correlation, as indicated, and the stars indicate the significance of the correlation.

Reporting Summary

Nature Portfolio wishes to improve the reproducibility of the work that we publish. This form provides structure for consistency and transparency in reporting. For further information on Nature Portfolio policies, see our [Editorial Policies](#) and the [Editorial Policy Checklist](#).

Statistics

For all statistical analyses, confirm that the following items are present in the figure legend, table legend, main text, or Methods section.

n/a Confirmed

- The exact sample size (n) for each experimental group/condition, given as a discrete number and unit of measurement
- A statement on whether measurements were taken from distinct samples or whether the same sample was measured repeatedly
- The statistical test(s) used AND whether they are one- or two-sided
Only common tests should be described solely by name; describe more complex techniques in the Methods section.
- A description of all covariates tested
- A description of any assumptions or corrections, such as tests of normality and adjustment for multiple comparisons
- A full description of the statistical parameters including central tendency (e.g. means) or other basic estimates (e.g. regression coefficient) AND variation (e.g. standard deviation) or associated estimates of uncertainty (e.g. confidence intervals)
- For null hypothesis testing, the test statistic (e.g. F , t , r) with confidence intervals, effect sizes, degrees of freedom and P value noted
Give P values as exact values whenever suitable.
- For Bayesian analysis, information on the choice of priors and Markov chain Monte Carlo settings
- For hierarchical and complex designs, identification of the appropriate level for tests and full reporting of outcomes
- Estimates of effect sizes (e.g. Cohen's d , Pearson's r), indicating how they were calculated

Our web collection on [statistics for biologists](#) contains articles on many of the points above.

Software and code

Policy information about [availability of computer code](#)

Data collection	Clinical data were recorded by a trained Clinical Research Associate using the Clinsight software (version _ Csonline 7.5.720.1). Flow Cytometry data were collected with BD FACSDIVA v8.01 or SpectroFlo V2.2.0 (Cytex)
Data analysis	Statistical analysis were performed using GraphPad Prism version 8. Flow Cytometry data were analyzed with FlowJo Software (10.6.1, FlowJo LLC, BD Life Sciences), GLM in R 4.1.0

For manuscripts utilizing custom algorithms or software that are central to the research but not yet described in published literature, software must be made available to editors and reviewers. We strongly encourage code deposition in a community repository (e.g. GitHub). See the Nature Portfolio [guidelines for submitting code & software](#) for further information.

Data

Policy information about [availability of data](#)

All manuscripts must include a [data availability statement](#). This statement should provide the following information, where applicable:

- Accession codes, unique identifiers, or web links for publicly available datasets
- A description of any restrictions on data availability
- For clinical datasets or third party data, please ensure that the statement adheres to our [policy](#)

The data that support the findings of this study are included in the "Source data" file available online.
Viral sequences are available on GISAID (GISAID accession numbers: EPI_ISL_1707038 19A (B.38) ; EPI_ISL_1707039 Alpha (B.1.1.7) ; EPI_ISL_768828 Beta (B.1.351) ; EPI_ISL_1359892 Gamma (P.1) ; EPI_ISL_1904989 ; Delta (B.1.617.2).

Field-specific reporting

Please select the one below that is the best fit for your research. If you are not sure, read the appropriate sections before making your selection.

Life sciences Behavioural & social sciences Ecological, evolutionary & environmental sciences

For a reference copy of the document with all sections, see [nature.com/documents/nr-reporting-summary-flat.pdf](https://www.nature.com/documents/nr-reporting-summary-flat.pdf)

Life sciences study design

All studies must disclose on these points even when the disclosure is negative.

Sample size	We did not perform sample size calculations as we did not know what to expect in terms of difference for the different measurements. We tried to analyze 30 patients in each group for all immunological measurements, as, based on our experience, it was sufficient to reach good statistics for most of the measurements, given that we minimize variability by selecting patients without comorbidity with similar age range, to avoid batch effects patients from each group (ie homologous vs heterologous) were included in each experiment and the number of experiments performed to test all samples was reduced as much as technically feasible.
Data exclusions	In the T cell experiments in Figure 3G-H we had to exclude several samples in both groups that were all analyzed on the same day. Indeed, for this particular day of experiment, the thawing step was not performed properly and cells died. Because only one PBMC sample was available for each donor, we could not repeat the experiments for the corresponding individuals. No other data were excluded in this study.
Replication	For all neutralization experiments two to three replicates were performed to ensure reproducibility. For commercial Elisa kits, internal quality controls ensure reproducibility. Attempts to replicate Elisa and neutralization experiments were all successful. For flow cytometry experiments, each patient was analyzed once. Samples were run on consecutive days, and the results were consistent over the different days, ensuring the validity of the measurements.
Randomization	Participants were health care workers. The participation of the study did not modify the vaccination schedule of each participant. The intervention on participants was limited to blood sampling. They were allocated in each group on the basis of their vaccination schedule (ie homologous vs heterologous). We recruited patients after the priming step, not before (we therefore did not decide which patients would receive each vaccine). The choice of the prime vaccine was only driven by the availability (both vaccines were approved and given without preference). For immunological assays, samples were blinded and randomized.
Blinding	For all experiments in Figures 2 and 3, we used a blinded strategy to perform immunological and serological analyses: Each sample was labelled with the reference (not the name) of the patient, but not the identity of the group (ie heterologous vs homologous vaccination) and the identity was only revealed at the analysis step, after blinded data acquisition.

Reporting for specific materials, systems and methods

We require information from authors about some types of materials, experimental systems and methods used in many studies. Here, indicate whether each material, system or method listed is relevant to your study. If you are not sure if a list item applies to your research, read the appropriate section before selecting a response.

Materials & experimental systems

n/a	Involved in the study
<input type="checkbox"/>	<input checked="" type="checkbox"/> Antibodies
<input type="checkbox"/>	<input checked="" type="checkbox"/> Eukaryotic cell lines
<input checked="" type="checkbox"/>	<input type="checkbox"/> Palaeontology and archaeology
<input checked="" type="checkbox"/>	<input type="checkbox"/> Animals and other organisms
<input type="checkbox"/>	<input checked="" type="checkbox"/> Human research participants
<input type="checkbox"/>	<input checked="" type="checkbox"/> Clinical data
<input checked="" type="checkbox"/>	<input type="checkbox"/> Dual use research of concern

Methods

n/a	Involved in the study
<input checked="" type="checkbox"/>	<input type="checkbox"/> ChIP-seq
<input type="checkbox"/>	<input checked="" type="checkbox"/> Flow cytometry
<input checked="" type="checkbox"/>	<input type="checkbox"/> MRI-based neuroimaging

Antibodies

Antibodies used

Pseudovirus neutralization assays:
Anti-spike SARS-CoV-2 RBD (Sino Biologicals # 40150-V08B2) 1/100
anti-gp70 RD114 (ViroMed Biosafety Labs, #RD114) 1/100

Elisas
Recombinant protein Spike S1-His: SARS-CoV-2 (2019-nCoV) -Cat: 40591-V08H (Sino-biologicals) coating 1 microgr/ml
Goat Anti-human IgA (alpha chain specific)-HRP (SIGMA)--Cat: A0295-1ML dilution 1/10000
Purified form of human chimeric IgA anti-RBD of SARS-COV-2 clone IB3C4 (B Cell Design): different concentrations (standard)

Flow cytometry:

Marker	Species/targeting	Fluorochrome	Clone	Supplier	Cat number	Dilution
CD28	mouse anti-human	purified	CD28.2	BioLegend	302933	1:100
CD49d	mouse anti-human	purified	9F10	BioLegend	304339	1:100
CD3	mouse anti-human	BV786	UCHT1	BD Biosciences	565491	1:100
CD4	mouse anti-human	BUV496	SK3	BD Biosciences	612937	1:50
CD8	mouse anti-human	PECy7	RPA-T8	BioLegend	301012	1:100
CD19	mouse anti-human	APC Cy7	HIB19	BioLegend	302218	1:100
CD14	mouse anti-human	APC Cy7	M5E2	BioLegend	301820	1:100
CD56	mouse anti-human	APC Cy7	5.1H11	BioLegend	362512	1:100
IFN γ	mouse anti-human	PE	B27	BD Biosciences	554701	1:50
Fixable Viability Dye		eF780		eBioscience	65-0865-14	1:500
CD3	mouse anti-human	APCFire810	SK7	Biolegend	344858	1:100
CD11c	mouse anti-human	BV785	3.9	Biolegend	301644	1:50
CD19	mouse anti-human	PE Vio770	LT-19	Miltenyi	130-113-170	1:100
CD20	mouse anti-human	BV421	2H7	BD Biosciences	562873	1:100
CD21	mouse anti-human	BUV496	B-ly4	BD Biosciences	750614	1:50
CD27	mouse anti-human	PercP-Vio700	M-T271	Miltenyi	130-113-632	1:100
CD38	mouse anti-human	Viobright FITC	REA572	Miltenyi	130-113-433	1:50
IgD	mouse anti-human	BV605	IA6-2	Biolegend	348232	1:50
IgM	mouse anti-human	PE-CF594	G20-127	BD Biosciences	562539	1:50
IgG	mouse anti-human	BV480	G18-145	BD Biosciences	746341	1:50

Biotinylated recombinant RBD domain of SARS Cov 2 RBD was purchased from Miltenyi Biotech (# 130-127-457) and tetramerized either with streptavidin-PE (BD Biosciences, # 554061) or with streptavidin-APC (Biolegend, # 105243).

Validation

All antibodies used in this study are commercially available, and all have been validated and quality checked by the manufacturers and used in other published works (For references, refer to the supplier's websites :

<https://wwwbdbiosciences.com/en-eu>

<https://www.biolegend.com/>

<https://www.thermofisher.com/fr/fr/home/life-science/antibodies/ebioscience.html>

<https://www.miltenyibiotec.com/FR-en/>.

We also have personal experience of all these antibodies and based on this experience, we can assess the validity of the antibodies. We titrated these antibodies according to our own staining conditions of human PBMCs (usually 1-2 millions cells/100 microliters, 30 min at 4°C).

Eukaryotic cell lines

Policy information about [cell lines](#)

Cell line source(s)

Vero E6 cells (ATCC CRL-1586) and HEK293T cells (ATCC CRL-1573)

Authentication

We did not authenticate the cell lines, but such authentication is performed by the supplier (ATCC) as part of the quality control

Mycoplasma contamination

All cell lines were regularly screened and tested negative for mycoplasma using a commercial kit (Lonza MycoAlert kit) # LT07-418

Commonly misidentified lines
(See [ICLAC](#) register)

no commonly misidentified cell lines were used in the study

Human research participants

Policy information about [studies involving human research participants](#)

Population characteristics

Health care workers for COVID-19 vaccinated with Pfizer BNT162b2 and/or AstraZeneca ChadOx01ncov-19 vaccines were included in a prospective longitudinal cohort study conducted in the Hospices Civils de Lyon (Lyon, France). Demographic characteristics are depicted in Table 2.

Recruitment

For the epidemiological investigation in Figure 1 (N=13121), all subjects (health care workers) who were vaccinated with both regimens were included, without exclusion criteria. For the 60 subjects included in the immunological study, we selected 60 subjects who had not been infected by SARS-CoV-2 before vaccination, without comorbidity, and who gave their consent for the study. Written informed consent was obtained from all participants.

Ethics oversight

The use and analysis of data from the occupational health medical file was authorized after a regulatory declaration to the National Commission for Information Technology and Civil Liberties (CNIL) according to the reference methodology (declaration MR004 n° 20-121 of 30 april 2020).

Covid-ser-vac: ethics approval was obtained from the national review board for biomedical research in April 2020 (Comité de Protection des Personnes Sud Méditerranée I, Marseille, France; ID RCB 2020-A00932-37)

Note that full information on the approval of the study protocol must also be provided in the manuscript.

Clinical data

Policy information about [clinical studies](#)

All manuscripts should comply with the ICMJE [guidelines for publication of clinical research](#) and a completed [CONSORT checklist](#) must be included with all submissions.

Clinical trial registration	NCT04341142
Study protocol	We amended the first version of protocol (https://bmjopen.bmj.com/content/10/11/e041268) with the aim to include vaccinated HCWs _ favorable amendment obtained 15th January 2021 from the comité de Protection des Personnes Sud Méditerranée I, Marseille, France; ID RCB 2020-A00932-37).
Data collection	For analyses of infections (Figure1), Health Care Workers at the Lyon University hospital (HCL) who received each vaccination regimen were monitored for infections starting in January 2021 in both groups. Data in Figure 1 show the infections that occurred after the 14-days postboost period, up to the end of the recording (08/15/2021) For immunological analyses (Figures 2-3), clinical data were collected using the Clinsight software, during January-April 2021. . Blood samples were processed and stored at the Centre de Ressource Biologique Neurobiotec, 69500 Bron. Serological and immunological analyses were performed at the Lyon-Sud hospital or at the Centre International de recherche en infectiologie (CIRI) in Lyon.
Outcomes	For figure 1 (analyses of infections) the primary outcome was the infection status ie not infected vs infected. This was assessed by performing RT-PCR for SARS-CoV-2 upon contact with confirmed cases or upon symptoms onset. For figures 2 and 3, (covid-ser study), the primary outcome was the positivity of the SARS-Cov-2 serological test at different time points, and the secondary outcome was the serum level of IgM and IgG titers and the serum neutralization capacity.

Flow Cytometry

Plots

Confirm that:

- The axis labels state the marker and fluorochrome used (e.g. CD4-FITC).
- The axis scales are clearly visible. Include numbers along axes only for bottom left plot of group (a 'group' is an analysis of identical markers).
- All plots are contour plots with outliers or pseudocolor plots.
- A numerical value for number of cells or percentage (with statistics) is provided.

Methodology

Sample preparation	For T cell stimulation and staining: Cryopreserved PBMCs were thawed and rested overnight in RPMI 1640 medium supplemented with 10% FBS in 5% CO2 at 37°C. On the second day, cytokine-producing T cells were identified by intracellular cytokine staining (ICS): Briefly, the PBMCs were stimulated with individual peptides for 1 h in the presence of 1 µg/mL monoclonal antibodies against human CD28 (Biolegend) and CD49d (Biolegend) then for an additional 5h with GolgiPlug (brefeldin A, BD Biosciences), GolgiStop (monensin, BD Biosciences). Then a standard antibody staining was carried out: dead cells were first labelled with LIVE/DEAD™ Fixable eF780 dye (ThermoFisher) and then followed by surface antibody staining. Subsequently, Cytofix/Cytoperm kit (BD Biosciences) was used for permeabilizing the cells before staining the cells with antibodies against molecules expressed intracellularly. For SARS-CoV-2 RBD-specific B cells analysis : PBMC staining were clearly described in the methods section of the manuscript. Briefly, cryopreserved PBMCs were centrifuged and resuspended in PEB Buffer (PBS + 0.5% BSA and 2 mM EDTA) and incubated with Fc receptor block (Miltenyi 130-059) for 15 min at 4°C. Next, cells were washed in PEB and stained for 30 min in brilliant stain buffer at 4°C in the dark using surface antibodies with both the PE- and APC-conjugated recombinant RBD tetramers. Then, cells were washed in PEB, and resuspended in a PEB dilution of the fixable viability dye eFluor 780 (ebiosciences 65-0865-18). They were next washed and fixed in 4% paraformaldehyde (PFA) for 20 min at 4°C in the dark before a final wash and resuspension for flow cytometry analysis.
Instrument	BD LSRFortessa 5L (T cell) or Cytek Aurora spectral flow cytometer 5L (B cell)
Software	Flow cytometry data were collected with BD FACSDIVA v8.01 or SpectroFlo V2.2.0 (Cytek) and analyzed with FlowJo software version 10.7.1 (FlowJo LLC)
Cell population abundance	Bulk PBMC were used. No cell sorting was performed.
Gating strategy	Peptide-specific T cell subsets were identified via the following gating strategy: Viable lymphocytes were addressed by successive gating in SSC-A/FSC-A plot followed by excluding DUMP positive cells (dead cells, CD14, CD19, CD56) in a FSC-A/DUMP plot. Then, singlets were gated in a FSC-A/FSC-H plot and CD3+ T cells were gated in CD3/FSC-A plot. From CD3+ T cells, CD4+ and CD8+ T cells were gated in CD4/CD8 plots. Next, peptide-specific CD4 T cells were gated by plotting CD4/IFNγ and peptide-specific CD8 T cells were gated by plotting CD8/IFNγ. Gating strategy for RBD-specific B cell analysis is provided in the supplementary information file and cell population are defined. Briefly, successive gating were applied for single cells and viable cells. Then, B cells were gated as CD19+/CD3- cells.

Within the B cell gate, memory B cells (mBCs) were defined as non-naïve/non transitional B cells on the same biparameter CD27/IgD plot. Then, PE- (RBD#1) and APC- conjugated (RBD #2) SARSCoV2 RBD probes in B cell gate and memory B cell gate were gated in RBD#1/ RBD#2 plot. Unswitched (IgD+CD27+), and switched (csM, IgD-CD27+) RBD-specific memory B cells were defined. Next, IgG+ and IgG-/IgM switched RBD-binding memory B cells were defined based on the IgM/IgG plot.

Tick this box to confirm that a figure exemplifying the gating strategy is provided in the Supplementary Information.